Figure DR1. Location and geometry map of the clastic dikes in Ami'az Plain. The letter code denotes the dikes and the sedimentary layers sampled for AMS analysis. Following is the number of measurements (in brackets) for each site: Tn (46), To (42), Tga-upper and central sectors (12), Tgb-lower sector (6), Tm (5), T (8), Rb- Phase I, multi-injection dike (12), Rf- Phase II, multi-injection dike (15), Rg- Phase III, multi-injection dike (12), Q-center (15), Qa-pipe around the source layer (8), Qb- pipe around the source layer (4), Qc- pipe around the source layer (10), Q-up (11), Q-source layer (10), Tp (27), Tk (23), Pza- fine detritus layer (20).
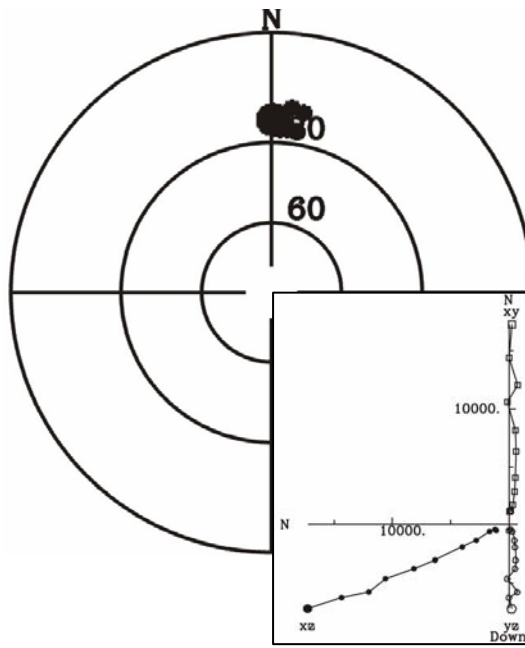
Figure DR2. Lower-hemisphere projection of natural remanent magnetization (NRM) directions and a vector-end point diagram of a representative clastic dike.
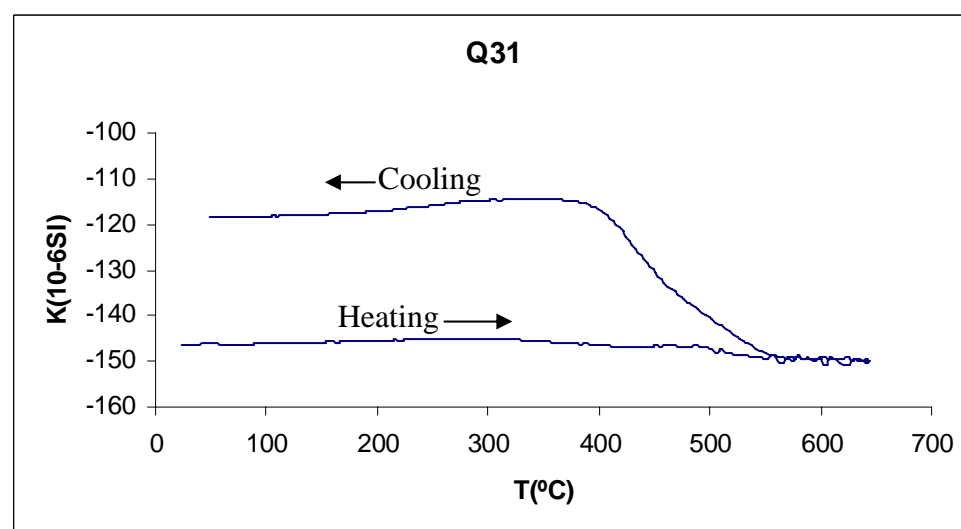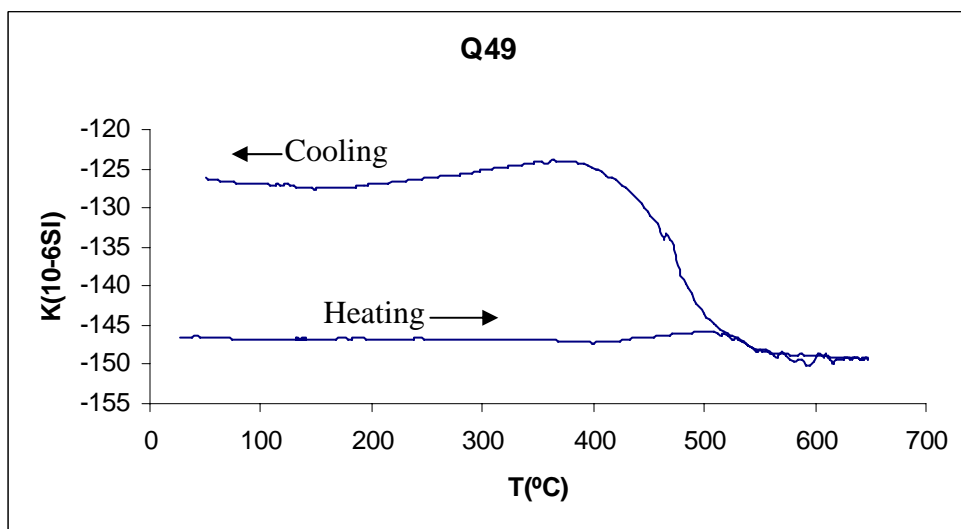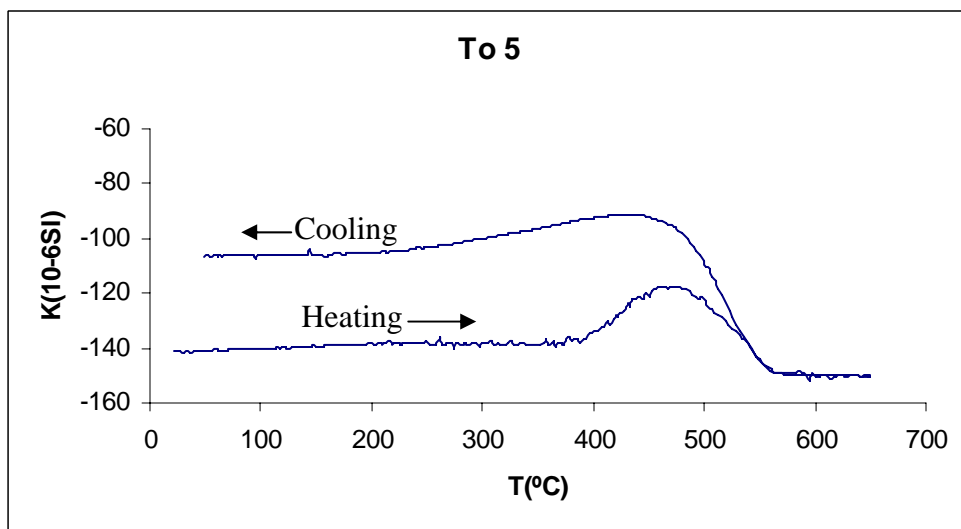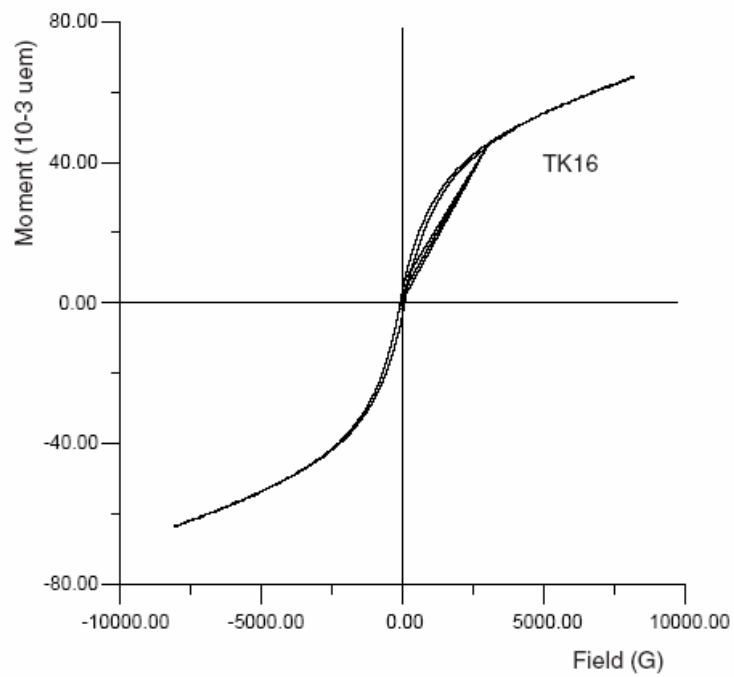
Figure DR3. Thermomagnetic curves for Neptunian dike (A, sample To5), Lisan source layer (B, sample Q49) and injection dike (C, sample Q31).
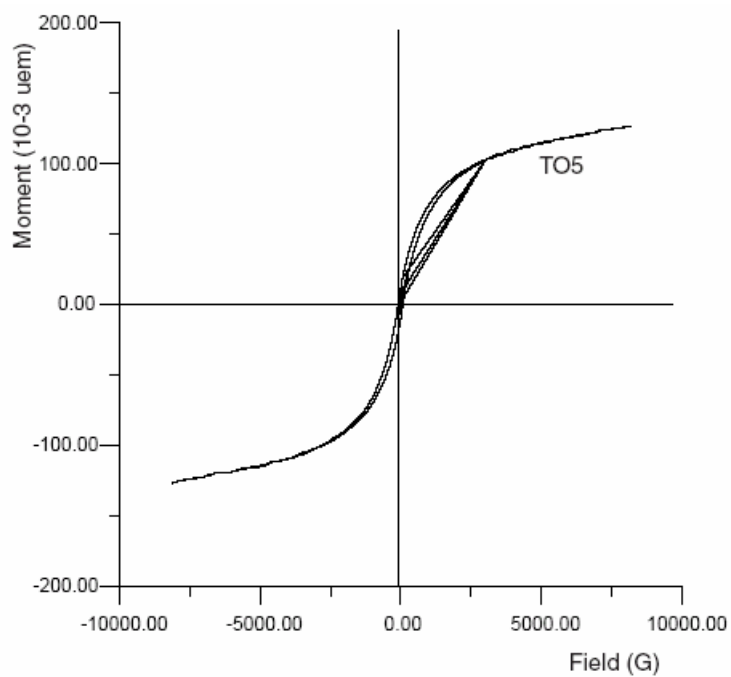
A.

B.

Figure DR4. Hysteresis loops for an injection dike (A, sample Tk16) and a Neptunian dike (C, sample To5).
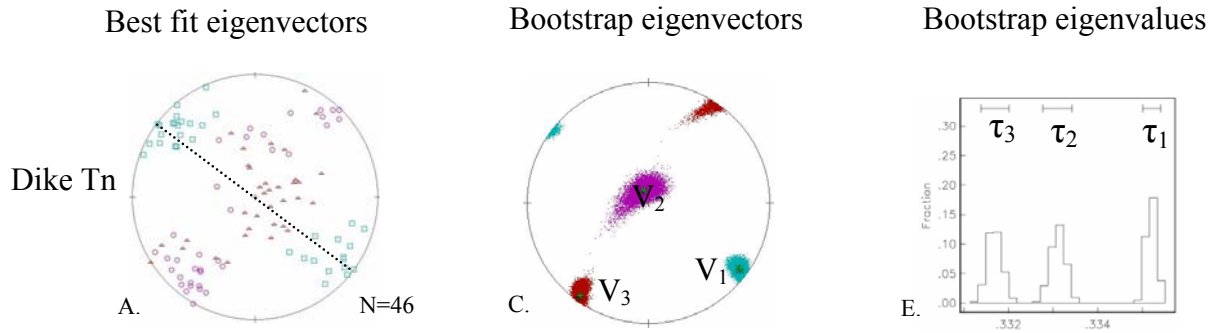
Figure DR5. Anisotropy of magnetic susceptibility (AMS) for a clastic dike (Dike Tn). A-B: Lower-hemisphere, equal-area projections of AMS eigenvector orientations; Squares are eigenvectors V_1, Triangles are eigenvectors V_2, and circles are eigenvectors V_3. C-D: Lower-hemisphere, equal-area projections of AMS eigenvector orientations bootstrapped AMS eigenvector distributions. E-F: Histograms of bootstrapped eigenvalues: τ_1, τ_2, and τ_3 with 95% confidence bounds. Broken lines mark the dike strikes. Dike Tn shows a streaked distribution of V_3 directions most likely formed during high flow velocity.